15 June 1996

OPTICS COMMUNICATIONS

ELSEVIER

Optics Communications 127 (1996) 215–222

Non-adiabatic effects in population transfer in three-level systems

N.V. Vitanov [1], S. Stenholm

Research Institute for Theoretical Physics, P.O. Box 9, (Siltavuorenpenger 20 C), University of Helsinki, 00014 Helsinki, Finland

Received 12 January 1996; accepted 7 March 1996

Abstract

We present an analytically solvable model for stimulated Raman adiabatic passage (STIRAP) processes in three-level systems. It involves *realistic* separated pulses which vanish at infinite times, whose pulse areas are finite and whose envelopes are smooth functions of time. The solution is obtained using the correspondence between three-level systems on resonance and two-level systems. The analytic model confirms the breakdown of the Dykhne-Davis-Pechukas exponential dependence of the non-adiabatic transition probability on the adiabaticity parameter found numerically recently.

PACS: 32.80; 33.80; 42.50

Keywords: Stimulated Raman adiabatic passage; Coherent population transfer; Three-level system

1. Introduction

In the recent years, stimulated Raman adiabatic passage (STIRAP) has rapidly become a subject of considerable theoretical and experimental interest. STIRAP is a very efficient and relatively simple technique for coherent population transfer in three-level Λ and 'ladder' systems. It requires three main conditions to be fulfilled (Fig. 1): *two-photon resonance, counter-intuitive pulse order* in which the Stokes pulse $\Omega_2(t)$ precedes the pump pulse $\Omega_1(t)$ though they overlap partly, and *adiabatic evolution*. Its particularly useful features are the insensitivity to changes of the pulse parameters over wide ranges and the stability against decay from the intermediate level. Various aspects of STIRAP have been studied theoretically [1–10] and experimentally [11]. A number of extensions of the three-level STIRAP have been considered, including effects of finite pulse bandwidth [2], decay [3,4], multiple intermediate or multiple final states [5], multilevel systems [6], and magnetic sublevels [3,7].

As far as the excitation is perfectly adiabatic, STIRAP guarantees *complete* population transfer from the initially populated level 1 to the final level 3. Not very much is known, however, about *how* the adiabatic limit is approached, that is about the probability of non-adiabatic transitions. This problem is of considerable theoretical interest because, as was shown very recently [8], for intermediate-level resonance, STIRAP reduces to a rather unusual effective two-level problem. Furthermore, numerical calculations [8] showed that the Dykhne-Davis-Pechukas (DDP) exponential dependence [12,8,9] of the probability for non-adiabatic transitions on the adiabaticity parameter may fail in the case of STIRAP. Moreover, this problem is of practical significance as well be-

[1] E-mail: nikolay.vitanov@helsinki.fi.

PII S0030-4018(96)00216-7

cause the excitation can never be made perfectly adiabatic.

The problem of non-adiabatic transitions could be understood much better if there were analytic solutions involving separated pulses. Such solutions have not been found so far for non-zero intermediate-level detuning δ, apart from the trivial case of rectangular pulses. The existing solutions [13] for three-level systems with $\delta \neq 0$, do not apply to STIRAP. Analytic solutions have only been derived in the case of intermediate-level resonance, $\delta = 0$ [10,8]. In these solutions, however, $\Omega_1(t)$ and/or $\Omega_2(t)$ have been either functions that do not vanish at infinity, which is physically impossible, or have been non-analytic functions.

In this paper, we show that, in the case of intermediate-level resonance, the Schrödinger equation *does* allow an exact analytic solution in which $\Omega_1(t)$ and $\Omega_2(t)$ are smooth realistic physical pulses. Our model shows explicitly that as the adiabaticity parameter increases the exponential DDP dependence of the deviation from perfect adiabatic transfer breaks into oscillations with an amplitude decreasing in a Lorentzian manner.

2. General background

2.1. The STIRAP mechanism

Consider a three-level Λ-system shown schematically in Fig. 1. The Schrödinger equation for the probability amplitudes in the rotating-wave approximation reads

$$i\frac{\mathrm{d}}{\mathrm{d}t}c(t) = \mathbf{H}(t)c(t), \tag{1}$$

where

$$\mathbf{H}(t) = \begin{bmatrix} 0 & \Omega_1(t) & 0 \\ \Omega_1(t) & \delta(t) & \Omega_2(t) \\ 0 & \Omega_2(t) & 0 \end{bmatrix} \tag{2}$$

and $c(t) = [c_1(t), c_2(t), c_3(t)]^{\mathrm{T}}$. The Rabi frequencies $\Omega_1(t)$ of the pump pulse and $\Omega_2(t)$ of the Stokes pulse are assumed positive without loss of generality. We suppose that at time $t \to -\infty$ the three-level system is in its ground state $|1\rangle$

$$c_1(-\infty) = 1, \quad c_2(-\infty) = 0, \quad c_3(-\infty) = 0, \tag{3}$$

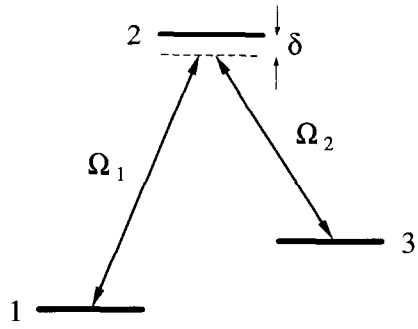

Fig. 1. The three-level Λ-system. Levels 1 and 2 are coupled by the pump laser pulse $\Omega_1(t)$ while levels 2 and 3 are coupled by the Stokes laser pulse $\Omega_2(t)$. The transition between levels 1 and 3 is electric-dipole forbidden. Levels 1 and 3 are on two-photon resonance while level 2 may be off resonance by the detuning δ. Only level 1 is populated initially. In STIRAP the Stokes pulse $\Omega_2(t)$ precedes the pump pulse $\Omega_1(t)$ (counterintuitive pulse order).

and we are interested in the populations at time $t \to +\infty$

$$P_n = |c_n(+\infty)|^2 \quad (n = 1,2,3). \tag{4}$$

The instantaneous eigenstates of the Hamiltonian $\mathbf{H}(t)$ are called *adiabatic* states. STIRAP exploits the existence of such an eigenstate which corresponds to the zero eigenvalue of $\mathbf{H}(t)$ and involves states $|1\rangle$ and $|3\rangle$ only

$$|0\rangle = \cos\vartheta(t)\,|1\rangle - \sin\vartheta(t)\,|3\rangle, \tag{5}$$

where

$$\tan\vartheta(t) = \frac{\Omega_1(t)}{\Omega_2(t)}. \tag{6}$$

In STIRAP the pulses are applied in counterintuitive order, that is the Stokes pulse $\Omega_2(t)$ *precedes* the pump pulse $\Omega_1(t)$, though they partly overlap. In other words,

$$\lim_{t\to-\infty}\frac{\Omega_1(t)}{\Omega_2(t)} = 0, \quad \lim_{t\to+\infty}\frac{\Omega_1(t)}{\Omega_2(t)} = +\infty, \tag{7}$$

which means that

$$\vartheta(-\infty) = 0, \quad \vartheta(+\infty) = \pi/2. \tag{8}$$

Hence, the adiabatic state $|0\rangle$ coincides with state $|1\rangle$ before the excitation and with state $|3\rangle$ after it, so that initially only state $|0\rangle$ among the adiabatic states is

populated. If *the excitation is adiabatic*, then the system will remain in this adiabatic state all the time and the population will eventually be completely transferred to state $|3\rangle$. Moreover, no appreciable population will reside in the intermediate state $|2\rangle$ at any time which makes the transfer efficiency insensitive to decay from this state to other states. We should note that as long as the adiabatic limit is concerned, STIRAP works irrespective of the value of the detuning δ. That is why we will assume $\delta = 0$ (intermediate-level resonance) in what follows, in order to enable an analytic treatment.

2.2. The effective two-level problem

For $\delta = 0$ the three-level problem is reduced to an effective two-level one with a detuning $\frac{1}{2}\Omega_2(t)$ and a coupling $\frac{1}{2}\Omega_1(t)$ [10,8]. In the adiabatic representation, the Schrödinger equation for this effective two-level system is [8]

$$i\dot{\mathbf{d}}(t) = \frac{1}{2}\begin{bmatrix} -\Omega_0(t) & -i\dot{\vartheta}(t) \\ i\dot{\vartheta}(t) & \Omega_0(t) \end{bmatrix} \boldsymbol{d}(t), \tag{9}$$

with the initial conditions

$$d_1(-\infty) = 1, \quad d_2(-\infty) = 0, \tag{10}$$

where $\boldsymbol{d}(t) = [d_1(t), d_2(t)]^{\mathrm{T}}$, $\vartheta(t)$ is given by Eq. (6),

$$\Omega_0(t) = \sqrt{\Omega_1^2(t) + \Omega_2^2(t)}, \tag{11}$$

and the dots mean time derivatives. In terms of the adiabatic two-level probability amplitudes $\boldsymbol{d}(t)$, the three-level amplitudes $\boldsymbol{c}(t)$ are given by [8]

$$\begin{aligned} c_1(t) &= \left[|d_1(t)|^2 - |d_2(t)|^2\right]\cos\vartheta(t) \\ &\quad + 2\mathrm{Re}[d_1(t)d_2^*(t)]\sin\vartheta(t), \\ c_2(t) &= -2i\,\mathrm{Im}[d_1(t)d_2^*(t)], \\ c_3(t) &= 2\mathrm{Re}[d_1(t)d_2^*(t)]\cos\vartheta(t) \\ &\quad - \left[|d_1(t)|^2 - |d_2(t)|^2\right]\sin\vartheta(t), \end{aligned} \tag{12}$$

and the initial conditions (10) ensure that the initial conditions (3) are satisfied. For counterintuitive pulses, $\vartheta(-\infty) = 0$ and $\vartheta(+\infty) = \pi/2$. Therefore, we have

$$\begin{aligned} c_1(+\infty) &= 2\mathrm{Re}[d_1(+\infty)d_2^*(+\infty)], \\ c_2(+\infty) &= -2i\,\mathrm{Im}[d_1(+\infty)d_2^*(+\infty)], \\ c_3(+\infty) &= |d_2(+\infty)|^2 - |d_1(+\infty)|^2. \end{aligned} \tag{13}$$

3. The analytic model

3.1. The pulses

The analytic model we are going to solve is defined by

$$\Omega_1(t) = \Omega_0(t)\sin\vartheta(t), \quad \Omega_2(t) = \Omega_0(t)\cos\vartheta(t), \tag{14}$$

with

$$\Omega_0(t) = \frac{\alpha}{\tau} f\left(\frac{t}{\sigma\tau}\right), \tag{15}$$

$$\vartheta(t) = \frac{\pi}{2}\frac{\arctan \mathrm{e}^{s(t)} - \arctan \mathrm{e}^{-\sigma}}{\arctan \mathrm{e}^{\sigma} - \arctan \mathrm{e}^{-\sigma}}, \tag{16}$$

where α, σ and τ are real positive parameters. Both α and σ are dimensionless while τ has the dimension of time and determines the time scale. The function $f(x)$ is an arbitrary non-negative function satisfying

$$\int_0^{\infty} f(x)\,\mathrm{d}x = 1, \tag{17}$$

and

$$s(t) = \frac{1}{\tau}\int_0^t f\left(\frac{t'}{\sigma\tau}\right)\mathrm{d}t' = \sigma\int_0^{t/\sigma\tau} f(x)\,\mathrm{d}x. \tag{18}$$

For simplicity we assume that $f(x)$ is an even function, $f(-x) = f(x)$; then, as time runs from $-\infty$ to $+\infty$, $s(t)$ changes from $-\sigma$ to σ. It is readily seen from (16) that $\vartheta(t)$ changes from 0 at $t \to -\infty$ to $\pi/2$ at $t \to +\infty$, which guarantees that the pulses $\Omega_1(t)$ and $\Omega_2(t)$ are applied in counterintuitive order. Furthermore, we require that $\Omega_1(t)$ and $\Omega_2(t)$ vanish at $t \to \pm\infty$ and their pulse areas are finite. Then $\Omega_0(t)$ is to be a pulse-shaped function too, because $\Omega_0(t) \leq \Omega_1(t) + \Omega_2(t)$. This condition is easily satisfied if the function $f(x)$ vanishes rapidly enough at infinity. Since the number of such functions $f(x)$ we can choose is infinite, the number of pairs $[\Omega_1(t),$

$\Omega_2(t)$] is infinite too. Thus, Eqs. (14)–(16) define a *class* of models rather than a single model with particular pulse shapes. As an example, one member of this class is obtained for the function $f(x)$ given by

$$f(x) = \operatorname{sech}^2 x. \tag{19}$$

Then

$$\Omega_0(t) = \frac{\alpha}{\tau} \operatorname{sech}^2 \frac{t}{\sigma\tau}, \tag{20}$$

$$\vartheta(t) = \frac{\pi}{2} \frac{\arctan e^{\sigma \tanh(t/\sigma\tau)} - \arctan e^{-\sigma}}{\arctan e^{\sigma} - \arctan e^{-\sigma}}. \tag{21}$$

The parameter α determines the pulse strengths and thus, α serves as the *adiabaticity parameter* in this model. The parameter σ controls the pulse shapes. In the limit $\sigma \to \infty$ this model reduces to an earlier model solved by Laine and Stenholm [8]

$$\Omega_1(t) = \frac{\alpha}{\tau} \frac{1}{\sqrt{1 + e^{-2t/\tau}}}, \quad \Omega_2(t) = \frac{\alpha}{\tau} \frac{1}{\sqrt{1 + e^{2t/\tau}}}. \tag{22}$$

In Fig. 2 we have plotted the pulse shapes corresponding to Eqs. (14) with $\Omega_0(t)$ given by (20) and $\vartheta(t)$ by (21) for σ equal to 1, 2, 4, 8, 12, and ∞. As σ increases the pulse areas increase too and become infinite for $\sigma \to \infty$.

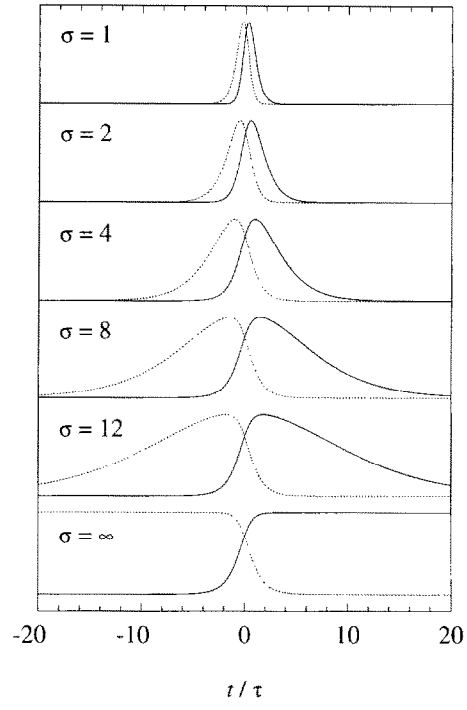

Fig. 2. The pulse shapes corresponding to Eqs. (14) with $\Omega_0(t)$ given by (20) and $\vartheta(t)$ by (21) for σ equal to 1, 2, 4, 8, 12, and ∞. In each case the pulses are applied in counterintuitive order: the Stokes pulses $\Omega_2(t)$, shown by dashed curves, precede the pump pulses $\Omega_1(t)$, shown by solid curves. As σ increases the pulse areas increase too and become infinite for $\sigma \to \infty$ (model (22)). For each σ, the pulse maxima are normalized (by changing α) to the same value.

3.2. The solution

The non-adiabatic coupling $\dot{\vartheta}(t)$ in our model defined by Eqs. (14) - (16) is

$$\dot{\vartheta}(t) = \frac{\beta}{\tau} f\left(\frac{t}{\sigma\tau}\right) \operatorname{sech} s(t), \tag{23}$$

where β is given by

$$\beta = \frac{\pi}{4\left[\arctan e^{\sigma} - \arctan e^{-\sigma}\right]} = \frac{\pi}{4 \arctan(\sinh \sigma)}. \tag{24}$$

To find the solution of Eqs. (9) for $\Omega_0(t)$ defined by (15) and $\dot{\vartheta}(t)$ given by (23), we change the independent variable from t to $s(t)$ and transform the probability amplitudes from $\boldsymbol{d}(t)$ to $\mathbf{D}[s(t)]$

$$\boldsymbol{d}(t) = \begin{bmatrix} 1 & 0 \\ 0 & i \end{bmatrix} \mathbf{D}[s(t)]. \tag{25}$$

Then Eqs. (9) take the form

$$i \frac{\mathrm{d}}{\mathrm{d}s} \mathbf{D}(s) = \tfrac{1}{2} \begin{bmatrix} -\alpha & \beta \operatorname{sech} s \\ \beta \operatorname{sech} s & \alpha \end{bmatrix} \mathbf{D}(s). \tag{26}$$

Therefore, the non-adiabatic coupling $\dot{\vartheta}(t)$ (23) and the eigenvalue splitting $\Omega_0(t)$ (15) in the present model are related to the coupling and the detuning in the well-known Rosen-Zener model [14]. There is, however, a substantial difference: in our model the variable s changes over a *finite* interval $[-\sigma, \sigma]$, while in the Rosen-Zener model the independent variable runs from $-\infty$ to $+\infty$. This leads to more complicated formulas for the probability amplitudes in the present case. The exact probability amplitudes at $s = \sigma$, that is at $t \to \infty$, are given by

$$D_1(\sigma) = -(1-i\alpha)\,e^{i\chi}\sqrt{\frac{1-p}{\alpha^2+1}}\,[F_1^*]^2 + \frac{2\beta}{1+i\alpha}\sqrt{p}\,\xi^{\frac{1}{2}+\frac{1}{2}i\alpha}(1-\xi)^{\frac{1}{2}-\frac{1}{2}i\alpha}F_1^*F_2 + \frac{\beta^2}{1+i\alpha}\xi^{1+i\alpha}(1-\xi)^{1-i\alpha}e^{-i\chi}\sqrt{\frac{1-p}{\alpha^2+1}}\,[F_2]^2, \tag{27}$$

$$D_2(\sigma) = -i\left\{\sqrt{p}\left[|F_1|^2 - \frac{\beta^2}{\alpha^2+1}\xi(1-\xi)\,|F_2|^2\right] + 2\beta\sqrt{\xi(1-\xi)}\sqrt{\frac{1-p}{\alpha^2+1}}\,\mathrm{Re}[e^{-i\varphi}F_1F_2]\right\}, \tag{28}$$

where $F_1 = F\left(\frac{1}{2}\beta, -\frac{1}{2}\beta; \frac{1}{2}+\frac{1}{2}i\alpha; \xi\right)$ and $F_2 = F\left(1+\frac{1}{2}\beta, 1-\frac{1}{2}\beta; \frac{3}{2}+\frac{1}{2}i\alpha; \xi\right)$ are short-hand notations for the Gauss hypergeometric function [15] and

$$\xi = \tfrac{1}{2}(1-\tanh\sigma) = \frac{1}{e^{2\sigma}+1}, \tag{29}$$

$$p = \sin^2\left(\tfrac{1}{2}\pi\beta\right)\mathrm{sech}^2\left(\tfrac{1}{2}\pi\alpha\right), \tag{30}$$

$$\chi = \arg\frac{\Gamma(\frac{1}{2}+\frac{1}{2}i\alpha)\Gamma(-\frac{1}{2}+\frac{1}{2}i\alpha)}{\Gamma(\frac{1}{2}-\frac{1}{2}\beta+\frac{1}{2}i\alpha)\Gamma(\frac{1}{2}+\frac{1}{2}\beta+\frac{1}{2}i\alpha)}, \tag{31}$$

$$\varphi = \chi - \frac{\alpha}{2}\ln\frac{\xi}{1-\xi}. \tag{32}$$

The solution (27) and (28) is derived in a similar way as in Refs. [14]. In the resulting expressions, hypergeometric functions of the arguments ξ and $1-\xi$ appear, rather than of the arguments 0 and 1 as in the Rosen-Zener model itself [14]. These expressions are then transformed by using standard properties of the hypergeometric functions to obtain (27) and (28). The latter equations are more convenient as they involve hypergeometric functions with arguments $\xi < \frac{1}{2}$ which decrease exponentially as σ increases. This improves considerably the accuracy of the approximations derived below utilizing the power-series expansions of the hypergeometric functions in (27) and (28). By keeping only the leading terms (equal to unity) of these expansions we obtain

$$|D_2(\sigma)|^2 \sim \left\{\sqrt{p}\,[1+O(\xi)] + 2\beta\sqrt{\xi}\sqrt{\frac{1-p}{\alpha^2+1}}\cos\varphi\;[1+O(\xi)]\right\}^2, \tag{33}$$

which is the non-adiabatic transition probability in the effective two-level system. According to Eqs. (13) the final population of level $|3\rangle$ is

$$P_3 = \left[2\,|D_2(\sigma)|^2 - 1\right]^2. \tag{34}$$

The populations of the other two levels in the three-level system can be obtained from (13), (27) and (28) too, but they lead to more complicated expressions which we do not present explicitly here. In the adiabatic limit, $|D_2(\sigma)|^2 = 0$ and the population transfer is perfect, $P_3 = 1$. The *deviation from perfect adiabatic transfer* is given by

$$\Delta P_3 = 1 - P_3 = 4\,|D_2(\sigma)|^2\left[1 - |D_2(\sigma)|^2\right]. \tag{35}$$

Eqs. (28) and (35) express the exact deviation from adiabatic transfer while Eqs. (33) and (35) give the approximation used in the analysis below.

3.3. Discussion

It is convenient to rewrite the deviation from adiabatic transfer (35) as a sum of two terms

$$\Delta P_3 = \Delta P_3^{(1)} + \Delta P_3^{(2)}, \tag{36}$$

where

$$\Delta P_3^{(1)} \sim 4p(1-p)\left[1 + O(\xi^{1/2})\right], \tag{37}$$

$$\Delta P_3^{(2)} \sim \frac{16\beta^2\xi}{\alpha^2+1}\cos^2\varphi\,[1+O(\xi)]. \tag{38}$$

These two terms are such that $\Delta P_3^{(1)}$ contains all p's, that is the exponentials of α, while $\Delta P_3^{(2)}$ contains rational functions of α only. The leading term of $\Delta P_3^{(1)}$ is of order $O(1)$ with respect to ξ but it is exponentially small with respect to α (via p). The leading term of $\Delta P_3^{(2)}$ is of order $O(\xi)$ with respect to ξ, that is exponentially small with respect to σ (see (29)), but it is of order $O(\alpha^{-2})$ with respect to α, rather than exponentially small. Hence, one expects that for finite and fixed ξ (that is for finite and fixed σ), $\Delta P_3^{(1)}$ dominates for small α while $\Delta P_3^{(2)}$ dominates for large α.

In the limit $\sigma \to \infty$, ξ is equal to zero; then $\Delta P_3^{(2)} = 0$ and the deviation from perfect transfer is given exactly by

$$\Delta P_3 = \Delta P_3^{(1)} = 4p\,(1-p) \quad (\sigma \to \infty). \tag{39}$$

For $\alpha \gg 1$, we have $\Delta P_3 \sim 16e^{-\pi\alpha}\sin^2(\pi\beta/2)$, that is ΔP_3 vanishes exponentially with the adiabaticity parameter α, in agreement with the DDP result. For *finite* σ, however, $\xi \neq 0$ and the term $\Delta P_3^{(2)}$ is non-zero; when α increases, it vanishes much more slowly (as α^{-2}) than $\Delta P_3^{(1)}$ and in an oscillatory manner. This implies that after a certain value of α, which we call the *DDP breakdown* value α_c, the term $\Delta P_3^{(2)}$ (38) overtakes the exponentially vanishing term $\Delta P_3^{(1)}$ (37) and becomes dominant. The deviation ΔP_3 is then given approximately by

$$\Delta P_3 \approx \Delta P_3^{(1)} \sim 4p(1-p) \quad (\alpha < \alpha_c), \tag{40}$$

$$\Delta P_3 \approx \Delta P_3^{(2)} \sim \frac{16\beta^2\xi}{\alpha^2+1}\cos^2\varphi \quad (\alpha > \alpha_c). \tag{41}$$

The DDP breakdown can clearly be seen in Fig. 3 where we have plotted the deviation from perfect transfer ΔP_3 as a function of the adiabaticity parameter α for σ equal to 1, 2, 4, 8 and 12, that is for the pulses shown in Fig. 2. In the figure, we compare the exact values (Eqs. (28) and (35)) with the approximate ones (Eqs. (33) and (35)); the latter coincide with the exact curves almost everywhere and can only be distinguished for $\sigma = 1$. For each σ, we have also shown the two terms $\Delta P_3^{(1)}$ and $\Delta P_3^{(2)}$ by short-dashed broken curves. The steeper dashed curve indicates the term $\Delta P_3^{(1)}$ (37), which is equal to the deviation for $\sigma \to \infty$ and dominates for small α, while the other dashed curve shows the amplitude of the oscillating term $\Delta P_3^{(2)}$ (38), which dominates for large α. The intersections between these two curves represent the DDP breakdown points α_c. These results clearly demonstrate that it is the finite value of σ, that is the *finite pulse area*, that makes the DDP exponential dependence fail. Actually, in the derivation of the DDP result [12], it is necessary to assume that the eigenvalues $\pm\frac{1}{2}\Omega_0(t)$ are non-degenerate at infinity. In the case of STIRAP, this is obviously not true; thus it is not surprising that the DDP derivation fails.

As we pointed out above, the DDP breakdown occurs at the point α_c where the term $\Delta P_3^{(1)}$ (37) is approximately equal to the amplitude of the oscillating term $\Delta P_3^{(2)}$ (38). For large σ, we can easily estimate the value of α_c. Then $\beta \approx \frac{1}{2}$ (see (24)) and $\sin^2\left(\frac{1}{2}\pi\beta\right) \approx \frac{1}{2}$. It is also readily seen that when σ is large, α must be large too. Thus, we find that for large σ the DDP breakdown occurs at

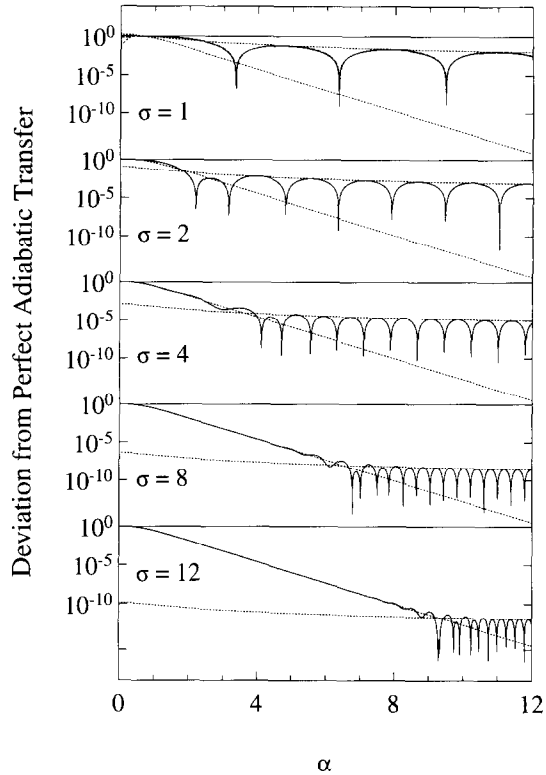

Fig. 3. The deviation from adiabatic transfer ΔP_3 as a function of the dimensionless adiabatic parameter α for σ equal to 1, 2, 4, 8 and 12, that is for the pulses shown in Fig. 2. The full curves represent the exact values (Eqs. (28) and (35)). The approximation (Eqs. (33) and (35)), shown by long-dashed broken curves, coincides with the exact curves almost everywhere and can only be distinguished for $\sigma = 1$. For each σ, the two short-dashed broken curves show the terms $\Delta P_3^{(1)}$ and $\Delta P_3^{(2)}$. The steeper dashed curve indicates the term $\Delta P_3^{(1)}$ (37), which is equal to the deviation for $\sigma \to \infty$ and dominates for small α, while the other dashed curve shows the amplitude of the oscillating term $\Delta P_3^{(2)}$ (38), which dominates for large α. The intersections between these two curves determine the DDP breakdown points α_c.

$$\sigma \approx \frac{\pi}{2}\alpha_c - \ln\left(\sqrt{2}\alpha_c\right), \tag{42}$$

which means that α_c is almost a linear function of σ. It turns out that an important parameter is the ratio R between the pulse areas and the overlap area of the two pulses. It can be shown that in the present model this ratio is approximately a linear function of σ for large σ (the approximate dependence, found numerically, is $R \approx 1.13\sigma + 0.79$). Then Eq. (42) means that the DDP breakdown value α_c is almost a linear

function of R. This conclusion is very similar to the results of Laine and Stenholm [8] based on numerical calculations for different pulse shapes (Gaussian and hyperbolic-secant; in Ref. [8], the pulse-area-to-overlap-area ratio has been controlled by keeping the pulse shapes the same and varying the pulse delay). A simple manipulation of the results in Table 3 of Ref. [8] for hyperbolic-secant pulses leads to the conclusion that the DDP breakdown value of their adiabatic parameter is approximately proportional to $R^{1.27}$.

We stress that an exponential region appears for large σ only (that is for large R) because then $\xi \sim e^{-2\sigma}$ is very small which makes the term $\Delta P_3^{(2)}$ (38) smaller than the term $\Delta P_3^{(1)}$ (37) over a large enough range of α (i.e. from zero to $\alpha_c \approx 2\sigma/\pi$). As we can see from Fig. 3, this is not the case for $\sigma = 1$ and $\sigma = 2$. A look at Fig. 2 confirms that for an exponential region to appear, the pulse-area-to-overlap-area ratio R should be large, in agreement with the conclusions of Laine and Stenholm [8]. A comparison of the curves for $\sigma = 8$ and $\sigma = 12$ in Fig. 3 reminds us of Figs. 11 and 12 in Ref. [8] where the oscillations are not shown.

4. Conclusion

We have presented an exact analytic solution describing STIRAP excitation for intermediate-level resonance. This model involves physically realistic separated pulses, that is pulses which vanish at infinite times, whose pulse areas are finite and whose envelopes are smooth analytic functions of time. To the best of our knowledge, this is the first such model to appear in the literature. The pulses contain two parameters: α determines the pulse strengths and thus plays the role of the adiabaticity parameter, while σ controls the pulse shapes. Our model shows explicitly that the exponential DDP dependence of the probability for non-adiabatic transitions breaks into oscillations as the adiabaticity parameter α increases. In the limit $\sigma \to \infty$, this model reduces to an earlier solved case involving pulses which do not vanish at infinity; in the latter case the DDP result is perfectly valid. These conclusions demonstrate clearly that it is the finite value of σ, that is the *finite pulse area*, which makes the DDP result fail because of the degeneracy of the eigenvalues at infinity. On the other hand, we have concluded that an exponential region can appear only when the pulse-area-to-overlap-area ratio R is large. We have also found that the DDP breakdown value of the adiabatic parameter α is almost a linear function of R. Finally, we should point out that the method we have implemented to find an analytic STIRAP solution by using the Rosen-Zener solution can be utilized to obtain additional solvable STIRAP models by using other available two-level solutions.

References

[1] F.T. Hioe and J.H. Eberly, Phys. Rev. Lett. 47 (1981) 838;
F.T. Hioe, Phys. Lett. A 99 (1983) 150;
J. Oreg, F.T. Hioe and J.H. Eberly, Phys. Rev. A 29 (1984) 690;
J. Oreg, J. Hazak and J.H. Eberly, Phys. Rev. A 32 (1985) 2776;
J.R. Kuklinski, U. Gaubatz, F.T. Hioe and K. Bergmann, Phys. Rev. A 40 (1989) 6741;
G.Z. He, A. Kuhn, S. Schiemann and K. Bergmann, J. Opt. Soc. Am. B 7 (1990) 1960;
B.W. Shore, K. Bergmann and J. Oreg, Z. Phys. D 23 (1992) 33;
B.W. Shore, K. Bergmann, A. Kuhn, S. Schiemann, J. Oreg and J.H. Eberly, Phys. Rev. A 45 (1992) 5297;
M.V. Danilenko, V.I. Romanenko and L.P. Yatsenko, Optics Comm. 109 (1994) 462.

[2] A. Kuhn, G. Coulston, G.Z. He, S. Schiemann, K. Bergmann and W.S. Warren, J. Chem. Phys. 96 (1992) 4215.

[3] Y.B. Band and P.S. Julienne, J. Chem. Phys. 94 (1991) 5291; 95 (1991) 5681; 96 (1992) 3339; 97 (1992) 9107;
Y.B. Band and O. Magnes, J. Chem. Phys. 101 (1994) 7528.

[4] B. Glushko and B. Kryzhanovsky, Phys. Rev. A 46 (1992) 2823.

[5] G. Coulston and K. Bergmann, J. Chem. Phys. 96 (1992) 3467.

[6] J. Oreg, K. Bergmann, B.W. Shore and S. Rosenwaks, Phys. Rev. A 45 (1992) 4888;
B.W. Shore, K. Bergmann, J. Oreg, and S. Rosenwaks, Phys. Rev. A 44 (1991) 7442;
A.V. Smith, J. Opt. Soc. Am. B 9 (1992) 1543.

[7] B.W. Shore, J. Martin, M.P. Fewell and K. Bergmann, Phys. Rev. A 52 (1995) 566;
J. Martin, B.W. Shore and K. Bergmann, Phys. Rev. A 52 (1995) 583.

[8] T.A. Laine and S. Stenholm, Phys. Rev. A 53 (1996) 2501.

[9] M. Elk, Phys. Rev. A 52 (1995) 4017.

[10] F.T. Hioe and C.E. Carroll, Phys. Rev. A 37 (1988) 3000;
C.E. Carroll and F.T. Hioe, J. Opt. Soc. Am. 5 (1988) 1335;
Phys. Rev. A 42 (1990) 1522.

[11] U. Gaubatz, P. Rudecki, M. Becker, S. Schiemann, M. Külz and K. Bergmann, Chem. Phys. Lett. 149 (1988) 463;
U. Gaubatz, P. Rudecki, S. Schiemann and K. Bergmann, J.

Chem. Phys. 92 (1990) 5363;
H.-G. Rubahn, E. Konz, S. Schiemann and K. Bergmann, Z. Phys. D 22 (1991) 401;
S. Schiemann, A. Kuhn, S. Steuerwald and K. Bergmann, Phys. Rev. Lett. 71 (1993) 3637;
P. Pillet, C. Valentin, R.-L. Yuan and J. Yu, Phys. Rev. A 48 (1993) 845.

[12] A.M. Dykhne, Zh. Eksp. Teor. Fiz. 38 (1960) 570 [Sov. Phys. JETP 11 (1960) 411]; 41 (1961) 1324 [14 (1962) 941];
J.P. Davis and P. Pechukas, J. Chem. Phys. 64 (1976) 3129.

[13] C.E. Carroll and F.T. Hioe, Phys. Rev. A 36 (1987) 724; J. Phys. B 22 (1989) 2633.

[14] N. Rosen and C. Zener, Phys. Rev. 40 (1932) 502;
N.V. Vitanov, J. Phys. B 27 (1994) 1351.

[15] M. Abramowitz and I.A. Stegun, eds., Handbook of Mathematical Functions (Dover, New York, 1964).